Long-term data reveal highly-variable metabolism and transitions in trophic status in a montane stream

Betsy M. Summers[1,6], David J. Van Horn[2,7], Ricardo González-Pinzón[1,8], Rebecca J. Bixby[2,9], Michael R. Grace[3,10], Lauren R. Sherson[4,11], Laura J. Crossey[4,12], Mark C. Stone[1,13], Robert R. Parmenter[5,14], T. Scott Compton[5,15], and Clifford N. Dahm[2,16]

[1]Department of Civil, Construction & Environmental Engineering, University of New Mexico, Albuquerque, New Mexico 87131 USA
[2]Department of Biology, University of New Mexico, Albuquerque, New Mexico 87131 USA
[3]Monash University, Water Studies Centre, Melbourne, Victoria, Australia
[4]Department of Earth and Planetary Sciences, University of New Mexico, Albuquerque, New Mexico 87131 USA
[5]Valles Caldera National Preserve, National Park Service, Jemez Springs, New Mexico 87025 USA

Abstract: In streams, gross primary production (GPP) and ecosystem respiration (ER) (i.e., stream metabolism) control the transport and fate of nutrients and organic carbon and vice versa. The importance of short-term and local factors in driving these processes is well known in the literature. However, little information exists regarding the extent of temporal variability of stream metabolism and how both local physicochemical and broad-scale climatic drivers affect this variability. We used 7 years of field data from an open-canopy headwater stream ecosystem in the southwestern United States to quantify the extent of seasonal and inter-annual variability in stream metabolism (GPP, ER, and net ecosystem production [NEP]) and to assess if temporal variation in these processes was related to the magnitude of snowmelt runoff. In spring, seasonal mean ER ($p = 0.025$, $r^2 = 0.67$) and NEP ($p = 0.004$, $r^2 = 0.83$) were more strongly related to discharge (Q) than GPP ($p = 0.19$, $r^2 = 0.32$), potentially because of an increased influx of nutrients and organic carbon during years with higher snowmelt runoff. There were no strong relationships between seasonal mean GPP and Q, light, temperature, turbidity, and specific conductance ($p \geq 0.27$, $r^2 \leq 0.18$). Our long-term data revealed unanticipated shifts from autotrophic to heterotrophic status within and across years. However, this variability was not strongly associated with environmental factors at either local (i.e., Q or photosynthetically-active radiation) or global (i.e., El Niño-Southern Oscillation) scales. Previous paradigms hold that local attributes dictated by geographic and landscape positioning (e.g., light and temperature regimes) control the trophic status of streams, but our findings suggest that complex combinations of spatiotemporally-variable factors, such as snow accumulation and melting, and their role in connecting terrestrial and aquatic ecosystems can lead to substantial within-stream variation in autotrophic or heterotrophic status.
Key words: stream metabolism, discharge, autotrophic, heterotrophic, trophic status, El Niño-Southern Oscillation, climate patterns

The production and consumption of oxygen and organic matter in streams both control and are controlled by the transport of nutrients and carbon. Thus, they have important implications for water quality of downstream lotic, lentic, and marine ecosystems. Daily oxygen and carbon production (via photosynthesis) and consumption (via autotrophic and heterotrophic respiration) can be estimated with diel dissolved oxygen curves and models of stream metabolism. These measurements are used to estimate both gross primary production (GPP) and ecosystem respiration (ER, the sum of autotrophic and heterotrophic respiration) (Odum 1956). Understanding the controls of GPP and ER in streams is essential for estimating how energy and nutrients flow through stream ecosystems (Hall and Tank 2003, Cohen et al. 2013, Hotchkiss and Hall 2015) and, consequently, many studies have focused on investigating predictors of spatial and temporal variation in stream metabolism (Mulholland et al. 2001, Bernot et al. 2010, Griffiths et al. 2013, Siders et al. 2017).

E-mail addresses: [6]bshafer3@unm.edu; [7]vanhorn@unm.edu; [8]gonzaric@unm.edu; [9]bbixby@unm.edu; [10]michael.grace@monash.edu; [11]lsherson@gmail.com; [12]lcrossey@unm.edu; [13]stone@unm.edu; [14]robert_parmenter@nps.gov; [15]scott_compton@nps.gov; [16]cdahm@unm.edu

DOI: 10.1086/708659. Received 22 July 2018; Accepted 2 November 2019; Published online 12 March 2020.
Freshwater Science. 2020. 39(2):000–000.

GPP and ER are controlled primarily by light, temperature, and disturbance and secondarily by nutrient and resource availability when the primary drivers are not limiting (Bernhardt et al. 2018). The study of these potential drivers in multiple and diverse biomes has provided insight into the mechanistic processes that affect stream metabolism. For example, the high light availability in open-canopy, semiarid streams supports higher rates of in-stream GPP relative to other stream types (Lamberti and Steinman 1997). Similarly, metabolic activity in the hyporheic zone, which is sustained by surface and groundwater inputs of dissolved organic carbon and nutrients, contributes to ER significantly more than other stream compartments (i.e., surface water) (Findlay et al. 1993, Mulholland et al. 1997, Naegeli and Uehlinger 1997, Fellows et al. 2001, González-Pinzón et al. 2014). Numerous short-term studies have provided valuable insights into the mechanisms driving metabolic regimes in streams. However, until recently, multi-year, high-resolution datasets necessary to assess seasonal and inter-annual variability and the factors driving these differences have been scarce.

The advent of low-cost water quality and nutrient sensors that are able to monitor almost continuously has begun to allow researchers to quantify long-term (e.g., seasonal and multi-year) variation in stream metabolism. Long-term monitoring allows researchers to infer how the relative influence of local drivers changes through time (Bernhardt et al. 2018). Additionally, by monitoring streams over multi-year time scales, it is becoming possible to document how large-scale global climate patterns influence stream metabolism. For example, one multi-year metabolism study found that GPP, ER, and net ecosystem production (NEP) varied by 5, 25, and 40%, respectively, between 2 consecutive years in a forested headwater stream (Roberts et al. 2007). Other multi-year studies in rivers in the western USA, Spain, and New Zealand have shown that the hydrologic variability resulting from management of flow, climate change (Marcarelli et al. 2010, Val et al. 2016), and geographic location (Young and Huryn 1996) were associated with fluctuations in daily and seasonal metabolism parameters.

To date, however, few long-term studies of stream metabolism have been conducted in the southwestern USA. In this region, the El Niño-Southern Oscillation (ENSO) phenomenon in the winter and spring and the North American monsoonal rainfall events in the summer influence both spatial and temporal variation in precipitation, and thus, stream discharge (Q). Specifically, El Niño (EN) years are often associated with increased regional snowpack, whereas La Niña (LN) years produce less snowpack, which influences snowmelt Q patterns (Molles and Dahm 1990). Additionally, the effects of climate change on ENSO are unknown (Collins et al. 2010), but snowpack in the western USA is decreasing because of warming air temperatures (Knowles et al. 2006). The strong linkages among global climate patterns, local precipitation, and the resultant stream flows make montane streams in the southwestern USA useful study sites for exploring inter-annual variability and the response of metabolism to large-scale climate drivers.

The overarching goals of this study were to quantify long-term temporal variability in metabolism within 1 site and assess how both local physicochemical and broad-scale climatic drivers might control this variability. We did this by collecting 7 y of growing-season field data from a snowmelt-dominated stream in north-central New Mexico, USA. We focused on 3 specific research questions that require long-term data: 1) how do GPP and ER vary seasonally and in conjunction with physicochemical variables typically linked to metabolism (i.e., water temperature, light, Q), 2) to what extent do seasonal and annual cumulative metabolism values and trophic status (autotrophy vs heterotrophy) vary, and 3) how does spring snowmelt Q influence metabolism? We hypothesized that: 1) both GPP and ER should peak during summer months in association with higher photosynthetically-active radiation (PAR), 2) trophic status will be similar across years (net autotrophic) because of the lack of riparian vegetation and abundance of incoming radiation in this montane grassland, and 3) disturbance from high-snowmelt EN years will reduce spring GPP and ER because higher flows likely scour the biological communities residing on or in benthic sediments, but high spring flows will not influence summer and autumn values.

METHODS

Study site

The East Fork Jemez River (EFJR) is located in the Jemez Mountains in north-central New Mexico, USA (Fig. 1). It is a low-gradient, high-sinuosity, high-elevation (~2590 m), 3rd-order perennial stream in the Valles Caldera National Preserve (VALL). The EFJR has an average base Q ranging from 0.06 to 0.09 m^3/s and a topographical gradient that ranges from near 0 to 7%. At our study reach, the stream gradient is ~0.05%, and streambed substrates consist of silt and organic matter in pools and gravel and cobble in riffles (Simino 2002). The stream channel is oriented from north to south, with a typical stream bank elevation of ~0.8 m and a slightly-incised channel.

Several landscape, climatic, and physicochemical attributes potentially influence GPP and ER at the study site. Vegetation in the river valley mainly consists of montane grassland, whereas Ponderosa pine (*Pinus ponderosa*) and mixed conifer forests dominate higher elevations within the catchment. The riparian vegetation in our study reach is sedge-dominated (*Carex* spp.) grassland. No trees or shrubs occur, which results in an open canopy over the stream. The annual growing season ranges from March to November, and peak primary production usually occurs between May and August for both aquatic and terrestrial primary producers.

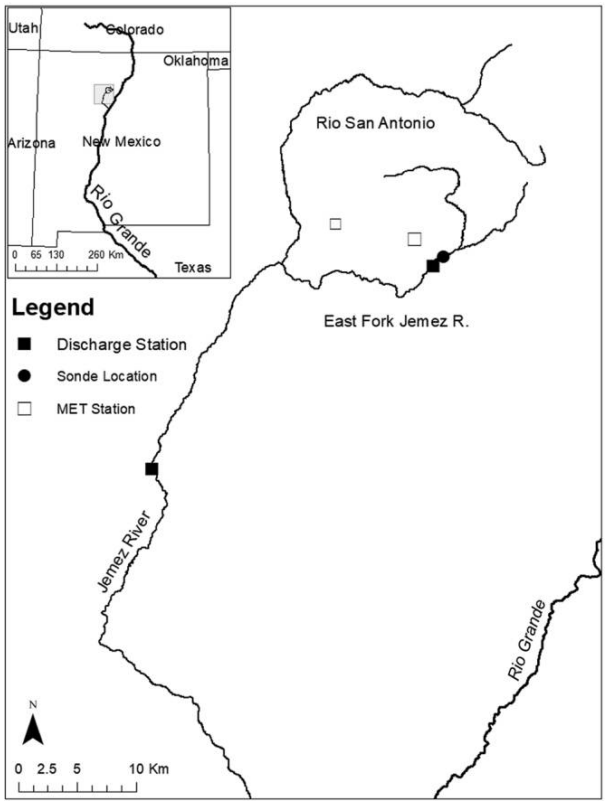

Figure 1. Location of study stream (East Fork Jemez River) and nearby meteorological and discharge sites in the Valles Caldera National Preserve and Jemez River in north-central New Mexico, USA.

Benthic algal assemblages increase in biomass immediately following snowmelt and remain active throughout the growing season. Additionally, the biomass of the 2 dominant submerged macrophyte taxa (*Elodea canadensis* and *Ranunculus aquatilis*) increases between the onset of spring (April–May) through early autumn (September–October), with mean total macrophyte biomass estimates ranging from 56 to 158 g ash free dry mass/m^2 throughout the growing season (Thompson et al. 2019). Previous solute injection experiments have identified nitrogen as the limiting nutrient for primary production in this stream (Van Horn et al. 2012).

Precipitation in the EFJR watershed is typically bimodal because of winter snowfall and summer monsoons. Data from the United States Geographical Survey (National Water Information System; https://waterdata.usgs.gov/nwis) stream gauge 08324000 on the Jemez River (main stem) downstream from the confluence of the EFJR and Rio San Antonio show that spring snowmelt greatly influences peak Q in years with a substantial snowpack. The timing and magnitude of snowmelt for the Jemez Mountains is also influenced by ENSO climate patterns. Specifically, EN years typically produce higher peak and total Q from snowmelt than LN years (Molles and Dahm 1990) (Fig. 2A). Summer monsoon storms affect stream Q by causing short, discrete peak discharges that occur primarily in July and August (Fig. 3A). These storms also create cloud cover, which increases the daily variability in PAR.

Data collection and external sources

We synchronized datasets of nearly continuous water quality and other environmental variables collected from 2005 to 2011 to generate long-term estimates of daily metabolism parameters. From this long-term record, we quantified the variability of metabolism rates at different time scales. We examined if GPP and ER varied in response to temporal changes in both local-scale physicochemical variables (Q, PAR, water temperature, turbidity, specific conductance) and global-scale variables (ENSO), and we identified shifts in trophic status at seasonal and annual time scales.

Water quality We measured dissolved oxygen (DO, mg/L), water temperature (°C), pH, turbidity, and specific conductivity (mS/cm) at 15-min intervals with a YSI 6920 water quality sonde (Yellow Springs, Ohio). The sonde was installed in the EFJR in 2005 at an elevation of 2583 m (site coordinates: lat 35°50′49.45″N, long 106°29′31.09″W). The sonde was operated yearly from April to November by the VALL (2005–2011) and the New Mexico Experimental Program to Stimulate Competitive Research (2010–2012, http://sevlter.unm.edu/node/1507). The sonde sensors were maintained and calibrated regularly (~once/mo) to reduce biofouling and ensure data quality. The DO probe was upgraded from a membrane-based probe to an optical probe in April 2011. We processed the raw data with Aquarius Workstation 3.3 (Aquatic Informatics, Vancouver, British Columbia), which allowed us to apply corrections for biofouling and calibration drift and delete spurious data when necessary.

Meteorology Measurements of PAR (μmol m^{-2} s^{-1}), atmospheric pressure, and air temperature (°C) were collected at 30-min intervals between 2005 and 2011. We obtained these measurements from 2 nearby meteorological stations: 1) Headquarters (lat 35°51′30″N, long 106°31′16″W), which is 2.74 km northwest of the study site in the Valle Grande and operated by the VALL; and 2) the TA-6 flux tower (lat 35°51′41.21″N, long 106°19′10.56″W), which is ~16 km east of the study site and operated by Los Alamos National Laboratories. We interpolated the meteorological data from both datasets to match 15-min sampling intervals collected by the sonde with a cubic spline function from the *zoo* package (Zeileis and Grothendieck 2005) (all statistical analyses were done in RStudio version 1.2.1335; R Project for Statistical Computing, Vienna, Austria). We also corrected barometric

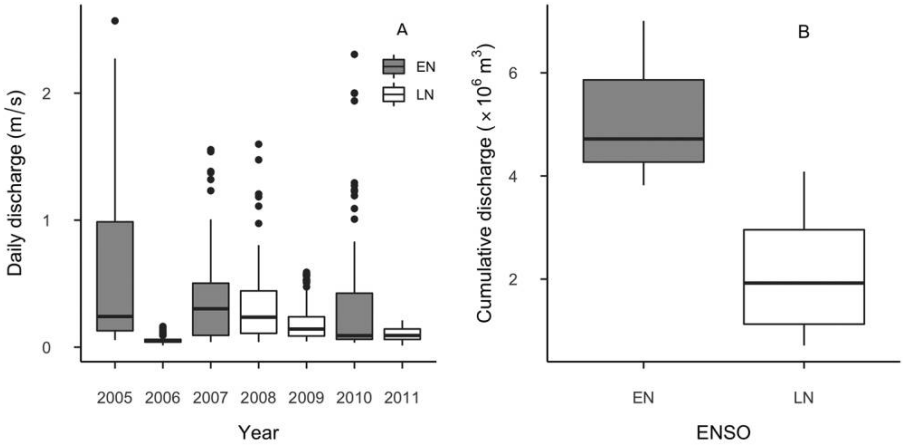

Figure 2. A.—Boxplots of the East Fork Jemez River (EFJR) daily discharge (m^3/s) during spring snowmelt from d 32 to 181 from y 2005 to 2011. B.—Cumulative discharge (m^3) for the snowmelt period grouped by the El Niño (EN, $n = 3$) and La Niña (LN, $n = 4$) years. The middle horizontal line represents the median in boxplots, the upper and lower lines represent the 1st and 3rd quartiles, and whiskers extend to the highest and lowest value within 1.5× the interquartile range.

pressure for elevation differences between the flux tower and study site with the hydrostatic equation (Barry and Chorley 2003). We used data from the Headquarters dataset whenever possible because it was closer to our study site and used the TA-6 dataset to fill gaps in the Headquarters dataset. We converted total solar irradiance (*SI*) in the dataset to PAR with the equation

$$\text{PAR} = \text{SI} \times 2.04 \qquad \text{(Eq. 1)}$$

(Meek et al. 1984). We then calculated the daily light integral from instantaneous measurements of PAR.

We assigned each study year to 1 of 3 ENSO categories (El Niño [EN], La Niña [LN], or Medial [M]). ENSO categories were defined based on 3-mo (December–February) running means of sea surface anomalies (see the Oceanic Niño Index from the National Oceanographic and Atmospheric Administration; http://elnino.noaa.gov/observ.html). Our study included 3 EN (2005, 2007, 2010) and 4 LN (2006, 2008, 2009, 2011) years. None of the years we studied were categorized as M.

Stream Q We estimated stream *Q* from daily discharge data recorded over the entire study period (2005–2011) at a downstream gauge (US Geological Survey stream gauge 08324000) located in the Jemez River near Jemez Pueblo, New Mexico (lat 35°39′43.14″N, long 106°44′36.38″W). This gauge is ~42 km downstream from our study site but has historically followed the same bimodal *Q* patterns driven by spring snowmelt and summer monsoons seen at the EFJR. We applied a widely-used hydrologic extrapolation technique for small watersheds that lack anthropogenic inflows to estimate *Q* at the EFJR (Q_{EFJRest}, m^3/s) reach (Gupta 2014). Equation 2 estimates Q_{EFJRest} as:

$$Q_{\text{EFJR}_{\text{est}}} = \frac{Q_{\text{JR}}}{A_{\text{JR}}} \times A_{\text{EFJR}}, \qquad \text{(Eq. 2)}$$

where Q_{JR} is daily average *Q* (m^3/s) measured for Jemez River, A_{JR} is the drainage area (1217 km^2) at the location where Q_{JR} is measured, and A_{EFJR} is the drainage area (115 km^2) for EFJR at the location where Q_{EFJRest} is estimated. To validate the accuracy of this extrapolation technique, we compared Q_{EFJRest} estimates with direct estimates of stream *Q* made at the EFJR site between 2008 and 2011. To directly estimate stream *Q*, we installed a near-streambed stilling well ~1.2 km downstream of our EFJR sonde site in April 2008. We deployed a water level logger (HOBO®, Onset®, Bourne, Massachusetts) in this well to record continuous stage measurements between 2008 and 2012. We used these data and 11 manual *Q* measurements (range: 0.05–1.7 m^3/s) collected between 2008 and 2012 ($r^2 = 0.97$; Fig. S1A) to develop a rating curve, which we used to estimate *Q* at the EFJR during the period between 2008 and 2012. Q_{EFJRest} was highly related with the estimates of *Q* based on the stilling well ($r^2 = 0.8$; Fig. S1B), so we used Q_{EFJRest} in all further analyses to maintain consistency in estimates of *Q* for the entire period with metabolism data (2005–2011).

Stream depth We estimated stage values with Q_{EFJRest} and the regression equation presented in Fig. S1A, such that

$$y_{\text{EFJR}} = -0.22Q_{\text{EFJR}}^2 + 0.73Q_{\text{EFJR}} + 0.15, \qquad \text{(Eq. 3)}$$

where stage y_{EFJR} is measured in m and Q_{EFJR} is measured in m^3/s. We validated the assumption that the estimated stage was representative of mean stream depth by referencing

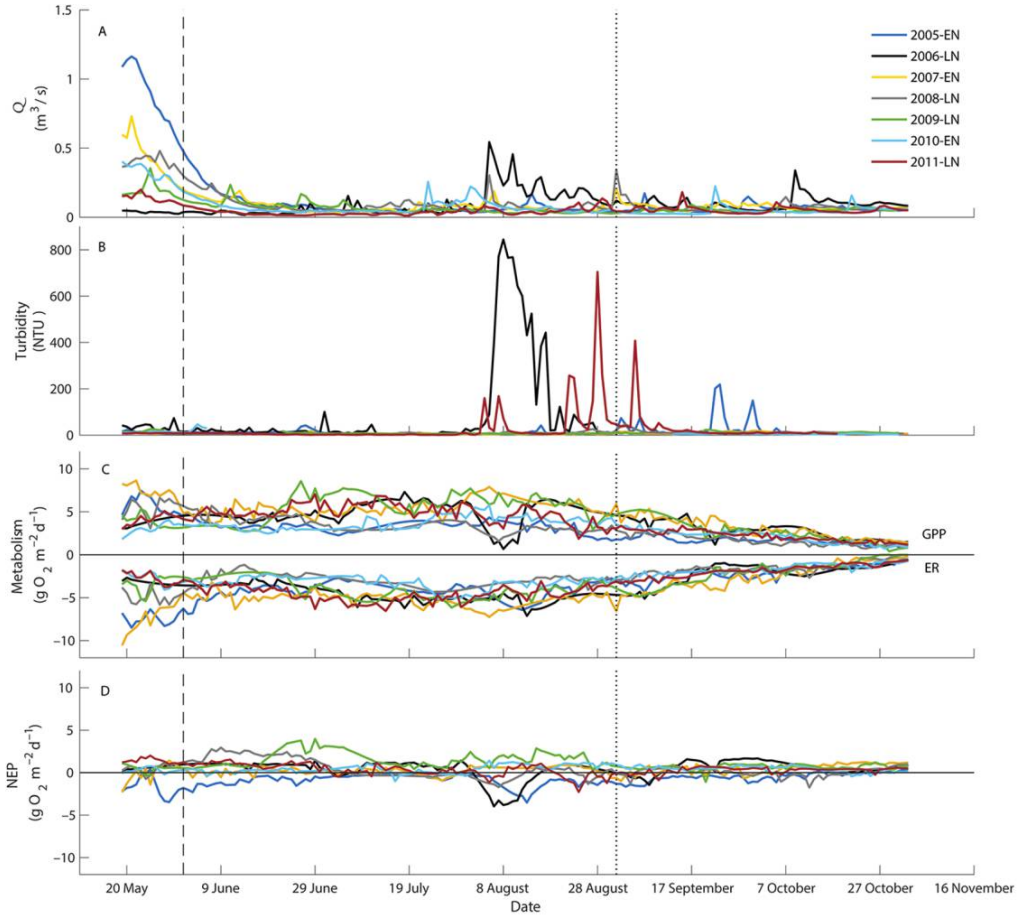

Figure 3. Time-series for daily measurements in the East Fork Jemez River from 2005 to 2011. Mean daily estimated discharge (Q, m^3/s) (A), turbidity (NTU) (B), daily gross primary production (GPP, g O_2 m^{-2} d^{-1}), ecosystem respiration (ER, g O_2 m^{-2} d^{-1}) (C), and net ecosystem production (NEP, g O_2 m^{-2} d^{-1}) (D). Measurements began 19 May and ended 2 November each year to span the growing season. Seasonal transitions are noted with a vertical dashed and dotted line for the beginning of summer and autumn, respectively.

field survey data previously collected by VALL (unpublished data) near the EFJR study site. These depths were measured in riffle, run, and pool habitats between 2006 and 2008 and again in 2010. We measured depth primarily in summer, when estimated Q ranged from 0.04 to 0.07 m^3/s. We found that the estimated stage and measured mean depth, averaged across habitats, were related ($r^2 = 0.69$, slope = 0.45, intercept = 0.10) along the reach (Fig. S1C). The root mean square error (0.012) indicates an average error of 1.2 cm associated with this assumption, which we considered negligible compared with other typical uncertainties in sensor data and modeling results (Aristegi et al. 2009).

Estimating GPP, ER, and reaeration

We estimated GPP, ER, and reaeration (K_{O2}, d) based on diel DO profiles and environmental variables (water temperature, specific conductivity as a surrogate for salinity, atmospheric pressure, and PAR) that we put into the Bayesian Single-station Estimation (BASE v2 released July 2016) modeling package (Grace et al. 2015). This approach used the following mass balance model:

$$[DO]_{t+1} = [DO]_t + AI_t^p - R\left(\theta^{(T_t-\bar{T})}\right) + K_{O_2} \times \left(1.0241^{(T_t-\bar{T})}\right) \times ([DO]_{\mathrm{sat},t} - [DO]_{\mathrm{mod},t}), \quad \text{(Eq. 4)}$$

where DO is the dissolved oxygen concentration (mg O_2/L) entered in time intervals of 15 min, A is a constant measuring primary production/quantum of light, and p describes the efficiency of light used and degree of saturating photosynthesis. PAR is represented as I (μmol m^{-2} s^{-1}) in this model. Together, PAR and A model parameters describe instantaneous primary production. Instantaneous respiration (R, mg O_2/L) is influenced by water temperature (T_t, °C), the

daily mean water temperature ($\overline{T}$, °C), and a coefficient for temperature dependence constrained to 1.072 (θ, 1/ °C). K_{O2} is estimated with saturated (sat) and modeled (mod) DO conditions. Instantaneous respiration and primary production rates were summed over a day to estimate daily ER and GPP (mg O_2 L^{-1} d^{-1}), respectively, then multiplied by stream depth to estimate fluxes of whole-stream metabolism (g O_2 m^{-2} d^{-1}). ER rates are expressed as negative values because ER consumes oxygen, with more negative values indicating higher respiration rates. BASE v2 also applies a salinity and temperature correction for DO saturation (Grace and Imberger 2006) and accounts for the temperature dependency of the respiration and reaeration constants with mean daily temperature during model fitting.

We set the number of Markov chain Monte Carlo (MCMC) iterations in the BASE v2 model to 100,000 with a burn-in of 50,000 iterations to estimate parameter values from the posterior probability distribution. We doubled the number of iterations if the MCMC chains did not converge to a stationary distribution. We used minimally-informative prior distributions for all parameters and estimated parameters for each discrete 24-hr period commencing at midnight. We used the model output to create a results table that included the model estimates of the mean value and uncertainty in each of the 4 parameters that describe daily metabolism (A, K_{O2}, R, and p), as well as the statistical criteria to assess model convergence and fit, as described in Grace et al. (2015). We used 3 statistical criteria to evaluate the daily model output included. First, $\widehat{R}$ measures the convergence of the MCMC chains. Values of $\widehat{R} < 1.1$ indicate convergence for all estimated parameters. Values of $\widehat{R} > 1.1$ were flagged as poorly mixed, rerun at the higher number of iterations described above, and visually checked with BASE-generated fitting plots. Second, the posterior predictive p-value measures whether model fits with respect to DO are adequate (~0.5) or inadequate (<0.1 or >0.9) while accounting for potential model discrepancies. Third, the association ($r^2 > 0.9$) between modeled and observed DO concentrations also assesses model fit (Gelman et al. 1996, Grace et al. 2015). There were 40 d for which $r^2 < 0.9$ and 76 d of poorly-fitting plots, which resulted in a total of 1328 d of good model fits out of 1444 daily runs. The relationship between ER and K_{O2} was assessed as diagnostic for equifinality (Fig. S2), and the relationship between GPP and the exponent p was assessed to better understand the behavior of GPP relative to available light (Fig. S3).

Interpolation of metabolism rates to compensate for time gaps

When model fits were poor or when time gaps occurred in data, we interpolated metabolism model results to generate a consecutive daily dataset to compare across-year trends in metabolism. We interpolated metabolism data because it required estimating only 2 missing values/d (GPP and ER), whereas interpolating DO values would have required us to estimate 96 missing values/d (24 h × 4 values/h). We used the dynamic harmonic regression function in the Captain toolbox (Taylor et al. 2007) for MatLab (version R2019a; MathWorks®, Natick, Massachusetts) to interpolate missing GPP and ER values for 28.7% of the total days. We did this by calibrating the noise variance hyperparameters (i.e., periodic behavior and model spectrum) used in the dynamic harmonic regression function iteratively with the Monte Carlo analysis toolbox (Wagener and Kollat 2007). This analysis minimized the root mean square error between the model generated by dynamic harmonic regression for a given year and the respective BASE v2 model simulations available. For time gaps >7 d, we constrained the model to the highest or lowest metabolism values available from other years (i.e., threshold rates) depending on whether the trend of daily data for that particular year was increasing or decreasing prior to the time gap. The longest time gap we filled was 40 d during July and early August in 2009. Single-day time gaps were filled with linear interpolation.

Data analysis

To answer research question 1, we analyzed time series data within and across years to identify seasonal and interannual trends in stream metabolism. We calculated the range in maximum values of daily GPP and ER within seasons to compare the magnitude and timing of biological activity within and across years. To identify potential drivers of seasonal variability in GPP and ER, we used simple, univariate linear regressions to test if seasonal mean estimates of metabolism parameters were related to Q, PAR, water temperature, turbidity, and specific conductivity.

We summed values of GPP and ER across seasonal and annual time periods using the same date range for each year to quantify the extent of seasonal and annual variability in cumulative GPP and ER (1st portion of research question 2). First, we calculated annual cumulative values between d 139 to 306 (19 May–2 November). Second, we calculated cumulative values for each season and year including spring (d 139–151; 19 May–31 May), summer (d 152–243; 1 June–31 August), and autumn (d 244–306; 1 September–2 November). We then took seasonal averages across years for the cumulative GPP and ER for spring, summer, and autumn and expressed the variability as the coefficient of variation (CV). We compared daily ER against GPP in relation to a 1:1 line across years to identify the trophic status (2nd portion of research question 2). A slope < -1 (more negative) suggests heterotrophic conditions were predominate and vice versa for autotrophic conditions (i.e., slope > -1). Additionally, we quantified NEP as the sum of GPP (positive) and ER (negative) and the percentage of days that autotrophy or heterotrophy persisted. Finally, we used linear regressions to determine if seasonal mean GPP and ER were related.

We did linear regressions between spring mean snowmelt *Q* and mean GPP, ER, and NEP to identify the response of GPP and ER to snowmelt *Q* (research question 3). We next estimated cumulative snowmelt *Q* for the period between d 32 and 151 and used 2 statistical tests to determine if ENSO varied with cumulative snowmelt *Q*. First, we used a 2-sample *t*-test to assess whether cumulative snowmelt *Q* differed between EN and LN groups and could thus be used as a proxy for ENSO category. Second, we regressed cumulative snowmelt *Q* on values of the Oceanic Niño Index. To test the potential linkage between metabolism parameters and large-scale climate patterns, we regressed spring cumulative ER, GPP, and NEP on the Oceanic Niño Index. We also used 2-sample t-tests to assess if GPP, ER, and NEP differed across ENSO categories.

We tested for normality and outliers in these data with Shapiro–Wilks tests and Q–Q plots (package *car*), Cook's distance, and the Bartlett test of homogeneity of variances for the *t*-test (Bartlett 1937). We report *p*-values as a continuous variable as suggested by Wasserstein et al. (2019). We used Spearman rank correlation to test for relationships between ER and *K* that can be indicative of equifinality (Fig. S2).

RESULTS

Variation in GPP and ER signals associated with seasonality and physicochemical variables

Seasonal differences in daily and average metabolism values

Maximum daily GPP values in the spring varied across years with low (4.0–5.3 g O_2 m^{-2} d^{-1}) values observed during some years (2006-LN, 2009-LN, 2010-EN, 2011-LN) and high (7.5–8.6 g O_2 m^{-2} d^{-1}) values in others (2005-EN, 2007-EN) (Fig. 3C). Maximum daily GPP values in summer also differed widely among years (4.9–8.6 g O_2 m^{-2} d^{-1}), and in some years (2005-EN, 2007-EN, 2008-LN) peak summer values were lower than peak spring values (Fig. 3C). At the onset of autumn, maximum daily GPP values ranged from 1.8 in 2005 to 5.9 g O_2 m^{-2} d^{-1} in 2007 and consistently declined with time, converging to similar low values (daily range: 0.8–1.5 g O_2 m^{-2} d^{-1}) by the end of the growing season (Fig. 3C).

During some years (2006-LN, 2010-EN, 2011-LN), maximum daily spring ER values were relatively low (–4.1 to −3.5 g O_2 m^{-2} d^{-1}) compared with other years (e.g., −10.6 to −8.5 g O_2 m^{-2} d^{-1} in 2005-EN and 2007-EN) (Fig. 3C). The range for the maximum summer daily rate of ER was smaller (–7.3 to −4.4 g O_2 m^{-2} d^{-1}) than that observed during spring. At the start of autumn, daily ER values were variable, ranging from −5.9 in 2007-EN to −2.6 g O_2 m^{-2} d^{-1} in 2008-LN. However, as with GPP, autumn ER values converged to similar lower or less negative values with time (daily values ranging −0.7 to 0.0 g O_2 m^{-2} d^{-1}; Fig. 3C).

In the spring, daily NEP values suggested heterotrophy in 2005-EN (–1.7 g O_2 m^{-2} d^{-1}) but autotrophy in nearly all other years (1.1–2.0 g O_2 m^{-2} d^{-1} in 2008, 2009-LN, 2010-EN, and 2011-LN) (Fig. 3D). NEP in 2007-EN was neither heterotrophic nor autotrophic (0.0 g O_2 m^{-2} d^{-1}). In the summer, daily NEP ranged between −4.0 in 2005-EN and 4.0 g O_2 m^{-2} d^{-1} in 2009-LN (both heterotrophic and autotrophic). Daily summer NEP values were more variable than those observed in spring. In early autumn, daily NEP values ranged between −1.3 in 2005-EN and 0.9 g O_2 m^{-2} d^{-1} in 2009-LN. Values were generally positive towards the end of autumn, converging to ~0.2 g O_2 m^{-2} d^{-1}.

We observed substantial variation in timing and magnitude of seasonal mean values of GPP and ER across years. Specifically, seasonal mean GPP and ER values were highest during spring or summer, depending on the year, and were consistently lowest in autumn (Table 1). Across all seasons, both minimum and maximum seasonal mean GPP values occurred in EN years (autumn of 2005 and spring of 2007, respectively). The minimum seasonal average ER occurred in an LN year (autumn of 2008) and the maximum occurred during an EN year (spring of 2005). Seasonal mean GPP and ER were more related in spring ($r^2 = 0.83$, $p = 0.004$, $n = 7$) and autumn ($r^2 = 0.57$, $p = 0.04$, $n = 7$) than in summer ($r^2 = 0.44$, $p = 0.1$, $n = 7$). Average NEP values in spring, summer, and autumn were 1.0 ± 2.1, 0.7 ± 0.3, and 0.4 ± 0.3 g O_2 m^{-2} d^{-1}, respectively.

Relationships between GPP, ER, and physicochemical variables

We found no clear relationships between seasonal mean water quality values (turbidity, specific conductivity, water temperature) and daily ER or GPP (Figs S4–S6) for spring, summer, or autumn (all *p*-values were >0.05, $n = 7$).

Variation in seasonal and annual cumulative metabolism values and trophic status

Seasonal cumulative GPP (Fig. 4B) for spring was more variable than across-year variation (CV = 31%; 40–96 g O_2/m^2 range bounded by 2010-EN and 2007-EN) for the summer (CV = 22%; 303–515 g O_2/m^2 range bounded by 2005-EN and 2009-LN) or autumn seasons (CV = 26%; 101–191 g O_2/m^2 range bounded by 2008-LN and 2007-EN). The highest cumulative annual GPP value (2007-EN 790 g O_2/m^2) was 49% higher than the lowest value (2005-EN 480 g O_2/m^2) (Fig. 4B).

Seasonal cumulative ER (Fig. 4B) for spring also had higher across-year variation (CV = 46%; −35 to −98 g O_2/m^2 range bounded by 2011-LN and 2005-EN) compared to summer (CV = 19%; −276 to −481 g O_2/m^2 range bounded by 2008-LN and 2007-EN) and autumn (CV = 17%; −97 to −160 g O_2/m^2 range bounded by 2008-LN and 2007-EN). Like GPP, the highest cumulative annual ER value (2007-EN: −737 g O_2/m^2) was ~50% higher than

Table 1. Seasonal gross primary production (GPP), ecosystem respiration (ER), and reaeration (K) mean values with standard deviations in parentheses from 2005 to 2011. Seasons were identified by day of the year: spring (139–151; 19 May–31 May), summer (152–243; 1 June–31 August), and autumn (244–306; 1 September–9 November). Range represents the overall minimum and maximum values across all seasons from 2005 to 2011.

		Mean (SD)		
Year	Season	GPP (g O_2 m^{-2} d^{-1})	ER (g O_2 m^{-2} d^{-1})	K (d)
2005-EN	Spring	5.79 (1.02)	7.50 (0.65)	6.02 (0.50)
	Summer	3.29 (0.63)	4.23 (0.99)	4.87 (0.96)
	Autumn	1.61 (0.43)	2.09 (0.85)	5.38 (1.46)
2006-LN	Spring	3.83 (0.36)	3.22 (0.21)	3.52[a] (NA)
	Summer	4.90 (1.61)	4.61 (1.35)	5.22 (1.95)
	Autumn	2.87 (0.95)	2.25 (1.50)	6.25 (0.79)
2007-EN	Spring	7.41 (0.43)	7.42 (1.19)	6.61 (0.58)
	Summer	5.46 (0.92)	5.22 (0.75)	5.50 (0.80)
	Autumn	3.04 (1.21)	2.54 (1.60)	5.83 (0.89)
2008-LN	Spring	5.56 (1.08)	5.00 (0.72)	7.48 (1.13)
	Summer	3.47 (0.90)	3.00 (0.70)	5.53 (0.81)
	Autumn	1.63 (0.61)	1.57 (0.77)	5.36 (0.77)
2009-LN	Spring	3.89 (1.88)	3.39 (1.35)	9.04 (1.98)
	Summer	5.60 (2.05)	3.99 (1.79)	6.84 (1.41)
	Autumn	2.74 (1.39)	2.08 (1.47)	5.79 (1.19)
2010-EN	Spring	3.05 (0.47)	2.76 (0.71)	6.45 (0.45)
	Summer	3.68 (0.76)	3.25 (0.76)	6.39 (0.86)
	Autumn	2.10 (0.80)	1.67 (0.61)	5.04 (1.08)
2011-LN	Spring	4.14 (0.48)	2.72 (0.66)	5.15 (0.68)
	Summer	4.91 (1.05)	4.58 (0.87)	5.69 (0.95)
	Autumn	2.18 (0.68)	1.88 (0.78)	4.71 (0.53)
2005–2011	Spring	4.81 (1.51)	4.57 (2.11)	6.53 (1.60)
	Summer	4.47 (0.97)	4.13 (0.79)	5.72 (1.27)
	Autumn	2.31 (0.58)	2.01 (0.34)	5.44 (1.05)
	Range	1.61–7.41	1.57–7.50	4.71–9.04

[a] K average is from 2 values in spring 2006. GPP and ER were interpolated. See methods for explanation.

the lowest values in 2008-LN and 2010-EN (both ~ −440 g O_2/m^2) (Fig. 4B).

Seasonal cumulative NEP ranged from −22 to 18 g O_2/m^2 in spring bounded by years 2005-EN and 2011-LN, −86 to 149 g O_2/m^2 in summer in 2005-EN and 2009-LN, and −30 to 39 g O_2/m^2 in autumn in 2005-EN and 2006-LN. Annual cumulative NEP ranged from −138 to 222 g O_2/m^2 in 2005-EN and 2009-LN, respectively. NEP during the growing season was positive in most years with autotrophic conditions being predominant in spring (75%, 69 of 92 d), summer (65%, 420 of 644 d), and autumn (71%, 312 of 440 d). However, heterotrophic conditions dominated in 2005-EN for spring (92%, 12 of 13 d), summer (99%, 91 of 92 d), and autumn (81%, 12 of 63 d).

Within each year, daily ER and GPP were strongly coupled, and their relationship was close to a −1:1 line (Fig. 5). However, this relationship diverged from the −1:1 line in spring 2005-EN and 2009-LN and in summer 2008-LN and 2009-LN. The slope of this relationship varied across years, ranging from −0.66 in 2009-LN ($r^2 = 0.77$) to −1.22 in 2005-EN ($r^2 = 0.83$). Only 2 of the 7 y had slopes < −1: 2005-EN (slope = −1.22, $r^2 = 0.83$) and 2007-EN (slope = −1.1, $r^2 = 0.9$).

Relationships between metabolism and spring snowmelt *Q*

Links between stream metabolism, Q, and ENSO Overall, mean ER and Q were linearly related in the spring ($r^2 = 0.67$, $p = 0.025$, $n = 7$; Fig. 6A). Mean NEP was strongly related to mean Q in spring ($r^2 = 0.83$, $p = 0.004$, $n = 7$; Fig. 6C). Rates of GPP tended to be higher with Q in spring ($r^2 = 0.32$, $p = 0.19$, $n = 7$; Fig. 6B), but this relationship was not as strong as those observed for ER and NEP.

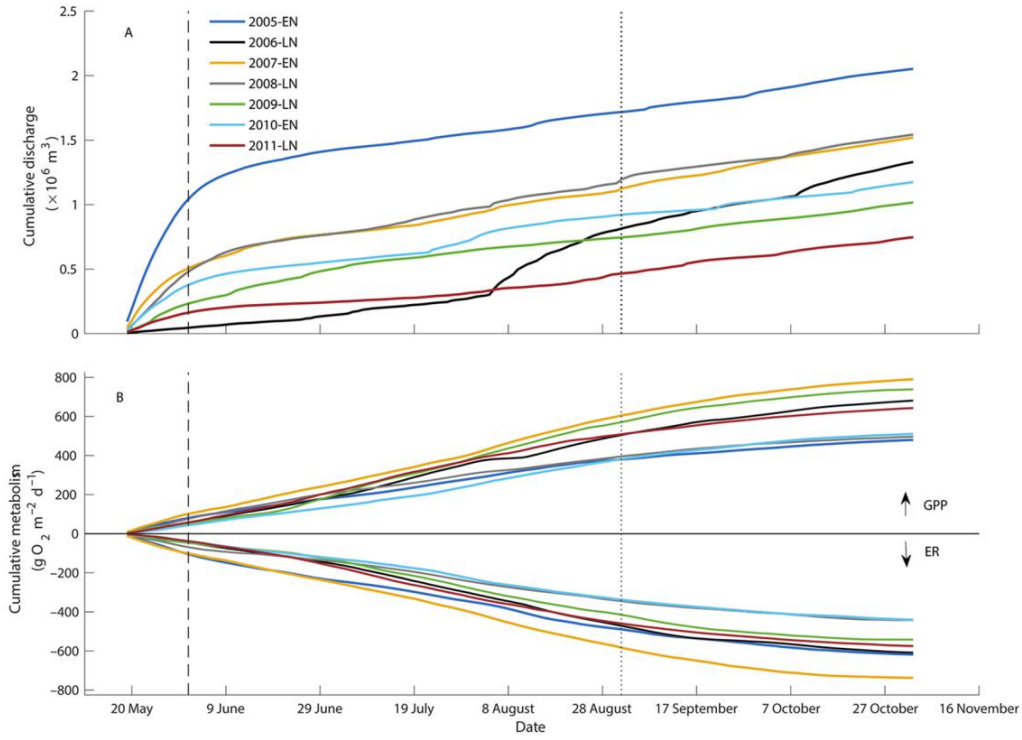

Figure 4. Time series of daily cumulative values of discharge (m^3) (A) and gross primary production (GPP, g O_2 m^{-2} d^{-1}) and ecosystem respiration (ER, g O_2 m^{-2} d^{-1}) (B) in the East Fork Jemez River. Seasonal transitions are noted with a vertical dashed line and dotted line for the beginning of summer and autumn, respectively.

A 2-sample *t*-test suggested that spring cumulative *Q* was higher in EN years (4.89×10^6 m^3) than in LN years (1.98×10^6 m^3) ($p = 0.048$, $n = 7$; Fig. 2B). However, spring cumulative ER, GPP, and NEP were not strongly related to an ENSO category.

DISCUSSION

In this open-canopy system, the timing of peak metabolism rates occurred in spring or summer. We found transitions in trophic status between heterotrophy and autotrophy at the sub-year and multi-year scale, which indicates that open-canopy streams can vary widely in the net production and consumption of carbon. In the spring, higher snowmelt runoff, which is associated with ENSO, was associated with enhanced ER rates and heterotrophic conditions. Together, these findings suggest that the variability of GPP and ER can be influenced by a complex combination of local and global drivers and may depend on the timescale measured.

Seasonal variation in metabolic signals and relationships to physicochemical variables

Spring The peaks in ER and GPP that occurred during spring in some years were contrary to our hypothesis that metabolism values would peak during summer months when PAR peaks. Springtime ER and GPP are typically highest prior to leaf emergence in streams in deciduous forests because of higher light availability (Acuña et al. 2004, Roberts et al. 2007). However, light availability is probably not responsible for the spring peak in metabolism in this stream because the riparian zone of the EFJR lacks woody vegetation and spring PAR was not significantly correlated with either GPP or ER (Fig. S4). An alternative driver could be snowmelt and its associated increase in erosion, which could prime metabolism by bringing more nutrients into the stream. While physical disturbances such as erosion can depress GPP and ER in some snowmelt-driven montane stream ecosystems (Uehlinger and Naegeli 1998), the minimal lateral scouring that occurs in this low-gradient (Fig. 3B), high sinuosity channel seems to mainly mobilize dissolved and readily bioavailable nutrients, allowing for higher springtime ER and GPP values. This finding suggests that one or more factors present during snowmelt stimulate pulses of production and respiration.

Our results align with the conceptual framework proposed by Bernhardt et al. (2018): that spring metabolism peaks in non-light-limited and low-disturbance systems result from an increased metabolic response to the snowmelt-induced provisioning of resources. A clear understanding of the underlying mechanisms responsible for these increases

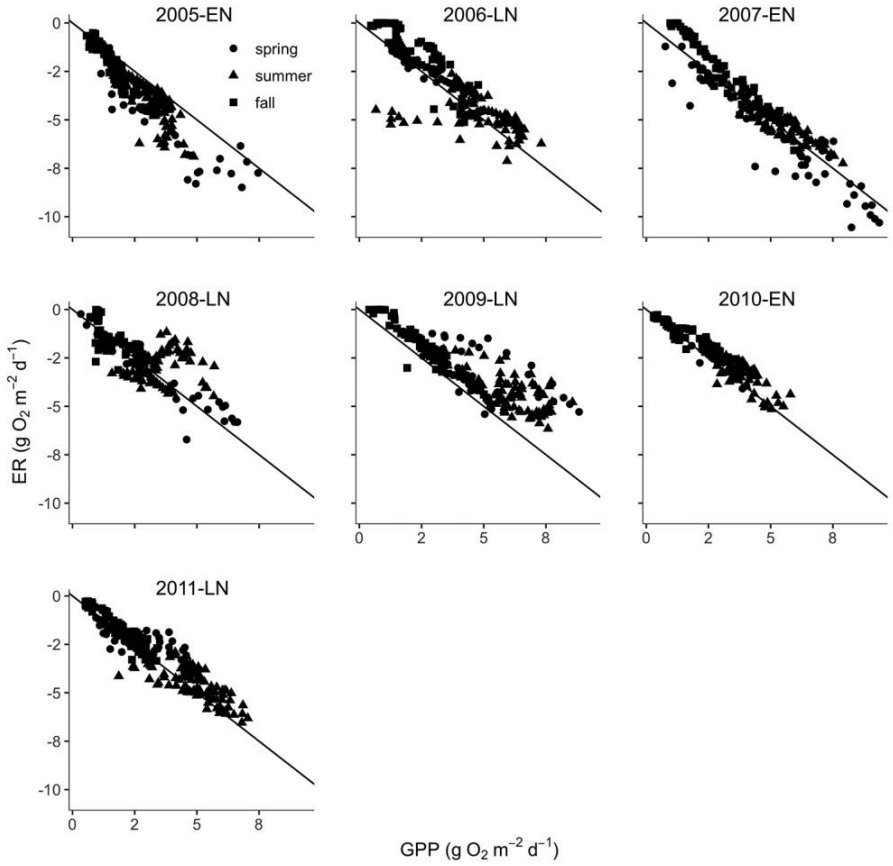

Figure 5. Ecosystem respiration (ER) vs gross primary production (GPP). This plot shows within-year shifts in heterotrophic and autotrophic conditions. The black line is the −1:1 line. Circles, triangles, and squares represent data points from the spring, summer, and autumn, respectively.

is lacking, but Demars (2019) found an increase of ER with snowmelt associated with the delivery of dissolved organic carbon from soils. Our study did not include continuous collection of inorganic nitrogen or dissolved organic carbon data, but studies in the EFJR and other streams support the hypothesis that in-stream nutrient concentrations increase from snowmelt and runoff events (e.g., Pellerin et al. 2012, Sherson et al. 2015). Precipitation events that cause small increases in *Q* can flush nitrate into the EFJR (Sherson et al. 2015). Other studies have also documented snowmelt-related inputs of nitrate (Pellerin et al. 2012) and dissolved organic carbon (Boyer et al. 1997) from near-stream environments, such as the zone of intermittent saturation and shallow alluvial aquifers (Valett et al. 1997, Baker et al. 2000). Furthermore, elevated flows convey organic matter into the hyporheic zone where it fuels heterotrophic organisms and increases ER (Metzler and Smock 1990). Similar increases in ER (and GPP) occur during spring flows in high-gradient alpine streams (Ulseth et al. 2018). Thus, we hypothesize that years with greater snowfall, which in this region depend on large-scale climate patterns, lead to greater spring flows that have a fertilization effect on stream metabolism. Testing this hypothesis requires the collection of regular nutrient and organic matter data in addition to metabolism estimates in the spring period.

Summer In general, ER and GPP declined in late spring and then slowly but steadily increased throughout the summer. This pattern probably occurred in response to inputs to the stream returning to baseflow following elevated spring flows as well as to subsequent increases in biomass production with increasing day length. Other open-canopy streams have a similar pattern of changes in metabolism (Roley et al. 2014). Abundant light availability in this system during summer promoted predominately-autotrophic conditions (65% of the summer). The strong linear relationship between daily ER and GPP for most years may be the result of autotrophic respiration, the dependence of heterotrophic activity on autochthonous organic carbon production, or a combination of both factors (Fig. 5). Autochthonous organic

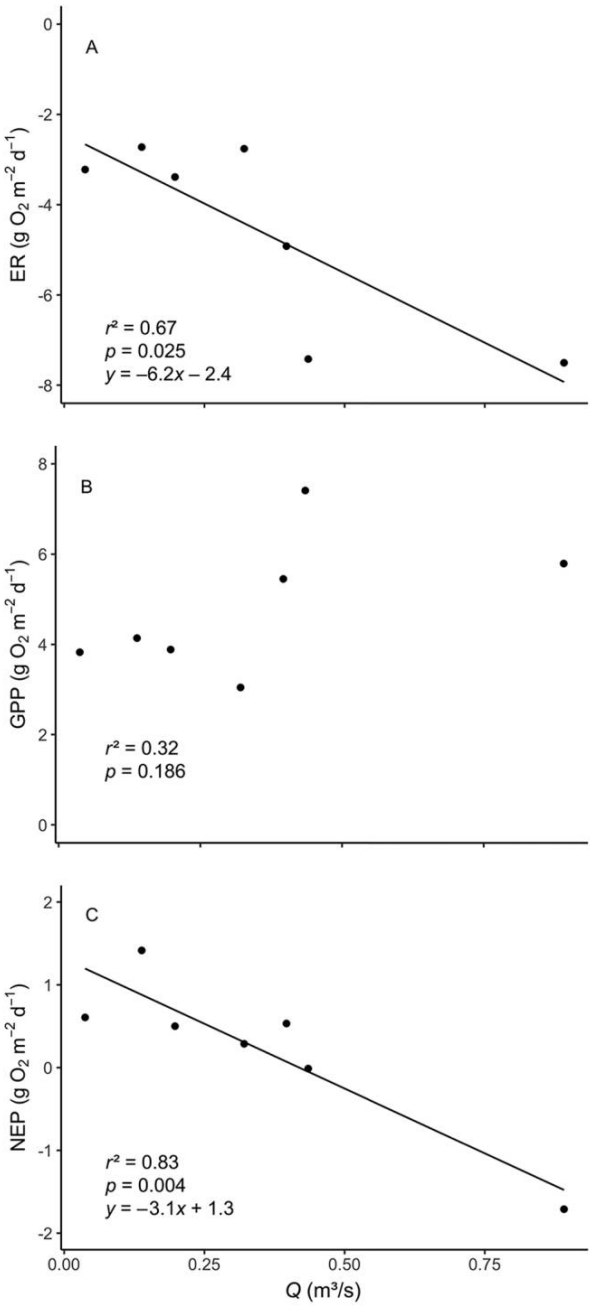

Figure 6. Mean spring (d 139 to 151) ecosystem respiration (ER) (A), gross primary production (GPP) (B), and net ecosystem production (NEP) (C) in g O_2 m^{-2} d^{-1} vs mean daily Q (m^3/s) during spring for y 2005 to 2011. ER and NEP are strongly related to Q. In contrast, GPP is not related with Q (r^2 = 0.32, p = 0.19, n = 7).

matter fuels ER in other open-canopy streams by causing the rapid heterotrophic uptake of algal exudates (Minshall 1978, Vannote et al. 1980, Hotchkiss and Hall 2015, Hall et al. 2016), which results in similar tightly-coupled daily ER and GPP values (Hotchkiss and Hall 2014, Hall et al. 2016, Arroita et al. 2019).

We found limited evidence for a positive relationship between PAR and GPP during the summer months (Fig. S5), even though the EFJR had high rates of primary production and PAR is expected to be a primary driver of GPP in open-canopy streams (Lamberti and Steinman 1997). This relationship likely did not occur in our study because this site is high elevation (~2590 m) and has long periods of direct sunlight, so light conditions are probably saturating and yield an asymptotic relationship between GPP and PAR (Young and Huryn 1996, Acuña et al. 2004). Furthermore, we found evidence of light saturation because the estimated p parameter averaged 0.5 and rarely approached a threshold of $p = 1.0$ that would indicate a linear relationship between GPP and PAR (Fig. S3). Alternatively, the lack of relationship between GPP and PAR could be the result of topographic shading by banks because the channel is moderately incised or by shading from the growth of riparian sedges and grasses during the summer months. We think channel topography may be particularly relevant because of the north–south orientation of the stream within the study reach, i.e., it can cause shading at sunrise and sunset, resulting in light limitation of primary production. Instances of substantial light limitation from increases in turbidity were only observed following a large flow event in 2006 and a catastrophic wildfire in 2011 (Dahm et al. 2015, Reale et al. 2015), which supports the hypothesis that erosive, overland flow events have a limited role in controlling metabolism in this relatively low-gradient grassland watershed.

Autumn As expected, GPP rates were lower in autumn than in spring or summer. However, contrary to our expectations, the trophic status in the EFJR did not shift from autotrophy to heterotrophy as it does in other lotic ecosystems (Uehlinger 2000, Griffiths et al. 2013). This difference may be related to the minimal allochthonous inputs in the EFJR relative to streams found in areas with deciduous forests (Roberts et al. 2007). Additionally, conditions in the EFJR remained favorable for primary production in autumn. Favorable conditions included high PAR because of minimal autumnal cloud coverage in New Mexico, limited surface ice formation because of relatively high day-time temperatures, minimal physical disturbance, tight coupling of GPP and ER, and efficient internal cycling of nutrients (Van Horn et al. 2012).

Variability in cumulative metabolism values and trophic status

Contrary to our original hypothesis, we found a high amount of variation in the ratio of GPP to ER, which resulted in shifts in the annual trophic status at our study site in the

EFJR. Annual NEP ranged from −138 in 2005 (heterotrophic) to 222 g O_2/m^2 in 2009 (autotrophic) (Fig. 5). The observed inter-annual shifts across heterotrophic, autotrophic, and neutral conditions show that variation in trophic status can occur even in hydrologically-stable streams with infrequent disturbance. Earlier predictions about stream metabolism in open-canopy, high-productivity streams suggested that they would be consistently autotrophic (e.g., Minshall 1978, Vannote et al. 1980). However, recent studies have found that these streams are most frequently heterotrophic (Hall et al. 2016). Thus, as suggested in other recent stream metabolism studies (Roberts et al. 2007, Beaulieu et al. 2013), our results show that within-stream variation in trophic status can be substantial at the sub-year and multi-year scale. Slopes ranged from −0.66 (heterotrophic) to −1.22 (autotrophic) (Fig. 5). Thus, streams cannot be accurately categorized as autotrophic or heterotrophic from brief snapshots taken in short-term stream metabolism studies. Instead, these classifications appear to depend strongly on the timescale over which metabolic rates are measured.

The drivers of this observed inter-annual variation in trophic status appear to be complex. Factors that influence one component of the metabolic regime (ER or GPP) may have either similar or opposite effects on the other component, resulting in either coupling or decoupling of the 2 signals. For example, ER appeared to be stimulated a few days earlier and to a greater extent than GPP in the largest spring snowmelt years (a difference of 1.03 in 2005-EN and 1.91 g O_2 m^{-2} d^{-1} in 2007-EN in terms of absolute values) in this study. This difference may have occurred because of an input of nutrients and organic matter resources from near-stream, organic-rich soils, as recently documented in other streams (Demars 2019). We suggest that this input causes a rapid heterotrophic response from the intact hyporheic community but a delayed and comparatively-muted response from the autotrophic community that has low benthic biomass in the spring. Similarly, Uehlinger (2006) found differential effects of disturbance on GPP vs ER that likely result from the partial physical separation of primary producers and heterotrophic communities in streams, i.e., primary producers are often found on benthic surfaces that receive incoming light, whereas heterotrophic organisms both co-occur with the primary producers and are also found in abundance in subsurface compartments and fine-grained pool sediments.

The drivers of year-end cumulative GPP and ER values appear to be similarly complex because metabolic peaks and troughs occurred throughout the year in this study. For example, years that had similar cumulative annual GPP and ER values appeared to be influenced by different drivers of metabolism, such as 2007-EN and 2009-LN (Fig. 4A–B). In the EFJR, we observed a large peak (multiple consecutive days with elevated values) in ER and GPP in the spring of 2007-EN, which was potentially linked to fertilization resulting from one of the largest snowmelt documented during this study. Additionally, a single large summer peak in GPP and ER occurred near the summer solstice of 2007, which probably was the result of increased solar radiation and temperatures (Fig. 3C). In contrast, there was a very small spring increase in ER and GPP in 2009-LN, probably because of the minimal snowpack-related runoff. However, 2 distinct peaks occurred during the summer for GPP and ER, likely because of a combination of reduced monsoonal-driven increases in Q and favorable light and water temperature conditions (Fig. 3A, C). Together, these results suggest that a wide variety of factors can lead to inter-annual variability in stream metabolism. Significant Q-related inter-annual variability in stream metabolism values has also been described in other montane, snowmelt-dominated streams that experience minimal scouring (Ulseth et al. 2018). High snowmelt years were correlated with increases in ER, likely related to resource inputs associated with snowmelt pulses (Ulseth et al. 2018). Thus, while our 7-y data set is long relative to previous studies, many additional years of observation, measurement of additional variables such as nutrients (Pellerin et al. 2012, Rode et al. 2016) and organic matter (Jones et al. 2014, Ruhala and Zarnetske 2017), and experimentation will be required to confidently link patterns to underlying mechanisms.

Linkages between stream metabolism and large-scale climatic patterns

Q and resource supply in high-elevation streams is often influenced by snowpack and subsequent snowmelt, creating a distinct hydro-climatic relationship. In the southwestern USA, this relationship is influenced by ENSO patterns (Molles and Dahm 1990, Pascolini-Campbell et al. 2015), which influences winter precipitation and subsequent snowmelt-related water resources. The relationship that we observed between ER and GPP values and the variation in ENSO-related total spring Q (i.e., higher volumes and increased duration for EN years relative to LN years) suggests that large-scale climate drivers can influence ER in the spring (Fig. 6A–C). The positive relationship that we observed between ER and snowmelt Q in spring, however, was contrary to our initial hypothesis that ER and GPP would be reduced during snowmelt. Ulseth et al. (2018) also found that inter-annual variability in the magnitude of snowmelt Q was associated with carbon cycling processes with shifts between export and mineralization during high- and low-flow years, respectively. Additionally, hydrologic models of climate change scenarios predict the timing of snowmelt will substantially enhance the inter-annual variation in in-stream carbon processing (Davis et al. 2013). Precipitation is increasingly shifting from snowfall to rainfall in the western USA as a result of climate change (e.g., Knowles et al. 2006), and snow is melting earlier in the year (Chavarria and Gutzler 2018). Thus, understanding the links between stream ecosystem function and global climate patterns will be an

important part of determining how climate change will affect the structure and function of stream ecosystems.

ACKNOWLEDGEMENTS

Author contributions: BS, DVH, and RGP wrote the manuscript; BS, DVH, LS, RP, and SC collected field data; BS, CD, DVH, RB, and RGP developed the research project; BS, MG, and RGP performed the modeling; CD, LC, MS, and RGP secured funding for the research. All authors contributed substantially to critical revisions of the manuscript and provided final approval for publication.

We appreciate feedback from Robert Hall and 2 anonymous reviewers on previous versions of this manuscript. Funding for this project was provided by the National Science Foundation through the New Mexico Experimental Program to Stimulate Competitive Research (EAR 0814449), through the Sevilleta Long-Term Ecological Research program (DEB 0620482), and through the Center for Water and the Environment (HRD-1345169).

LITERATURE CITED

Acuña, V., A. Giorgi, I. Muñoz, U. Uehlinger, and S. Sabater. 2004. Flow extremes and benthic organic matter shape the metabolism of a headwater Mediterranean stream. Freshwater Biology 49:960–971.

Aristegi, L., O. Izagirre, and A. Elosegi. 2009. Comparison of several methods to calculate reaeration in streams and their effects on estimation of metabolism. Hydrobiologia 635:113–124.

Arroita, M., A. Elosegi, and R. O. Hall. 2019. Twenty years of daily metabolism show riverine recovery following sewage abatement. Limnology and Oceanography 64:S77–S92.

Baker, M. A., H. M. Valett, and C. N. Dahm. 2000. Organic carbon supply and metabolism in a shallow groundwater ecosystem. Ecology 81:3133–3148.

Barry, R. G., and R. J. Chorley. 2003. Atmosphere, weather, and climate. 8th edition. Routledge, New York, New York.

Bartlett, M. S. 1937. Properties of sufficiency and statistical tests. Proceedings of the Royal Society of London. Series A: Mathematical and Physical Sciences 160:268–282.

Beaulieu, J. J., C. P. Arango, D. A. Balz, and W. D. Shuster. 2013. Continuous monitoring reveals multiple controls on ecosystem metaoblism in a suburban stream. Freshwater Biology 58: 918–937.

Bernhardt, E. S., J. B. Heffernan, N. B. Grimm, E. H. Stanley, J. W. Harvey, M. Arroita, A. P. Appling, M. J. Cohen, W. H. McDowell, R. O. Hall, J. S. Read, B. J. Roberts, E. G. Stets, and C. B. Yackulic. 2018. The metabolic regimes of flowing waters. Limnology and Oceanography 63:S99–S118.

Bernot, M. J., D. J. Sobota, R. O. Hall, P. J. Mulholland, W. K. Dodds, J. R. Webster, J. L. Tank, L. R. Ashkenas, L. W. Cooper, C. N. Dahm, S. V. Gregory, N. B. Grimm, S. K. Hamilton, S. L. Johnson, W. H. McDowell, J. L. Meyer, B. Peterson, G. C. Poole, H. M. Valett, C. Arango, J. J. Beaulieu, A. J. Burgin, C. Crenshaw, A. M. Helton, L. Johnson, J. Merriam, B. R. Niederlehner, J. M. O'Brien, J. D. Potter, R. W. Sheibley, S. M. Thomas, and K. Wilson. 2010. Inter-regional comparison of land-use effects on stream metabolism. Freshwater Biology 55: 1874–1890.

Boyer, E. W., G. M. Hornberger, K. E. Bencala, and D. M. McKnight. 1997. Response characteristics of DOC flushing in an alpine catchment. Hydrological Processes 11:1635–1647.

Chavarria, S. B., and D. S. Gutzler. 2018. Observed changes in climate and streamflow in the Upper Rio Grande Basin. Journal of the American Water Resources Association 54:644–659.

Cohen, M. J., M. J. Kurz, J. B. Heffernan, J. B. Martin, R. L. Douglas, C. R. Foster, and R. G. Thomas. 2013. Diel phosphorus variation and the stoichiometry of ecosystem metabolism in a large spring-fed river. Ecological Monographs 83:155–176.

Collins, M., S. An, W. Cai, A. Ganachaud, E. Guilyardi, F. Jin, M. Jochum, M. Lengaigne, S. Power, A. Timmermann, G. Vecchi, and A. Wittenberg. 2010. The impact of global warming on the tropical Pacific Ocean and El Niño. Nature Geosciences 3:391–397.

Dahm, C. N., R. I. Candelaria-Ley, C. S. Reale, J. K. Reale, and D. J. Van Horn. 2015. Extreme water quality degradation followig a catastrophic forest fire. Freshwater Biology 60:2584–2599.

Davis, J. M., C. V. Baxter, G. W. Minshall, N. F. Olson, C. Tang, and B. T. Crossby. 2013. Climate-induced shift in hydrological regime alters basal resource dynamics in a wilderness river ecosystem. Freshwater Biology 58:306–319.

Demars, B. O. L. 2019. Hydrological pulses and burning of dissolved organic carbon by stream respiration. Limnology and Oceanograph 64:406–421.

Fellows, C. S., H. M. Valett, and C. N. Dahm. 2001. Whole-stream metabolism in two montane streams: Contributions of the hyporheic zone. Limnology and Oceanography 46:523–531.

Findlay, S., D. Strayer, C. Goumbaba, and K. Gould. 1993. Metabolism of stream water dissolved organic carbon in the shallow hyporheic zone. Limnology and Oceanography 38:1493–1499.

Gelman, A., X.-L. Meng, and H. Stern. 1996. Posterior predictive assessment of model fitness via realized discrepancies. Statistica Sinica 6:733–807.

González-Pinzón, R., R. Haggerty, and A. Argerich. 2014. Quantifying spatial differences in metabolism in headwater streams. Freshwater Science 33:798–811.

Grace, M. R., D. P. Giling, S. Hladyz, V. Caron, and R. M. Thompson. 2015. Fast processing of diel oxygen curves: Estimating stream metabolism with BASE (BAyesian Single-station Estimation). Limnology and Oceanography: Methods 13:103–114.

Grace, M. R., and S. Imberger. 2006. Stream metabolism: Performing and interpreting measurements. Water Studies Centre Monash University, Murray Darling Basin Commission and New South Wales Department of Environment and Climate Change.

Griffiths, N. A., J. L. Tank, T. V. Royer, S. S. Roley, E. J. Rosi-Marshall, M. R. Whiles, J. J. Beaulieu, and L. T. Johnson. 2013. Agricultural land use alters the seasonality and magnitude of stream metabolism. Limnology and Oceanography 58:1513–1529.

Gupta, R. 2014. Hydrology and hydraulic systems. 3rd edition. Waveland Press, Long Grove, Illinois.

Hall, R. O., and J. L. Tank. 2003. Ecosystem metabolism controls nitrogen uptake in streams in Grand Teton National Park, Wyoming. Limnology and Oceanography 48:1120–1128.

Hall, R. O., J. L. Tank, M. A. Baker, E. J. Rosi-Marshall, and E. R. Hotchkiss. 2016. Metabolism, gas exchange, and carbon spiraling in rivers. Ecosystems 19:73–86.

Hotchkiss, E. R., and R. O. Hall. 2014. High rates of daytime respiration in three streams: Use of $\delta^{18}O$ and O_2 to model diel ecosystem metabolism. Limnology and Oceanography 59:798–810.

Hotchkiss, E. R., and R. O. Hall. 2015. Whole-stream ^{13}C tracer addition reveals distinct fates of newly fixed carbon. Ecology 96:403–416.

Jones, T. D., N. A. Chappell, and W. Tych. 2014. First dynamic model of dissolved organic carbon derived directly from high-frequency observations through contiguous storms. Environmental Science & Technology 48:13289–13297.

Knowles, N., M. D. Dettinger, and D. R. Cayan. 2006. Trends in snowfall versus rainfall in the western United States. Journal of Climate 19:4545–4559.

Lamberti, G. A., and A. D. Steinman. 1997. A comparison of primary production in stream ecosystems. Journal of the North American Benthological Society 16:95–104.

Marcarelli, A. M., R. W. Van Kirk, and C. V. Baxter. 2010. Predicting effects of hydrologic alteration and climate change on ecosystem metabolism in a western US river. Ecological Applications 20:2081–2088.

Meek, D. W., J. L. Hatfield, T. A. Howell, S. B. Idso, and R. J. Reginato. 1984. A generalized relationship between photosynthetically active radiation and solar radiation. Agronomy Journal 76:939–945.

Metzler, G. M., and L. A. Smock. 1990. Storage and dynamics of subsurface detritus in a sand-bottomed stream. Canadian Journal of Fisheries and Aquatic Sciences 47:588–594.

Minshall, G. W. 1978. Autotrophy in stream ecosystems. BioScience 28:767–771.

Molles, M. C., and C. N. Dahm. 1990. A perspective on El-Niño and La-Niña—Global implications for stream ecology. Journal of the North American Benthological Society 9:68–76.

Mulholland, P. J., C. S. Fellows, J. L. Tank, N. B. Grimm, J. R. Webster, S. K. Hamilton, E. Marti, L. Ashkenas, W. B. Bowden, W. K. Dodds, W. H. McDowell, M. J. Paul, and B. J. Peterson. 2001. Inter-biome comparison of factors controlling stream metabolism. Freshwater Biology 46:1503–1517.

Mulholland, P. J., E. R. Marzolf, J. R. Webster, D. R. Hart, and S. P. Hendricks. 1997. Evidence that hyporheic zones increase heterotrophic metabolism and phosphorus uptake in forest streams. Limnology and Oceanography 42:443–451.

Naegeli, M. W., and U. Uehlinger. 1997. Contribution of the hyporheic zone to ecosystem metabolism in a prealpine gravel-bed river. Journal of the North American Benthological Society 16: 794–804.

Odum, H. T. 1956. Primary production in flowing waters. Limnology and Oceanography 1:102–117.

Pascolini-Campbell, M. A., R. Seager, D. S. Gutzler, B. I. Cook, and D. Griffin. 2015. Causes of interannual to decadal variability of Gila River streamflow over the past century. Journal of Hydrology: Regional Studies 3:494–508.

Pellerin, B. A., J. F. Saraceno, J. B. Shanley, S. D. Sebestyen, G. R. Aiken, W. M. Wollheim, and B. A. Bergamaschi. 2012. Taking the pulse of snowmelt: In situ sensors reveal seasonal, event and diurnal patterns of nitrate and dissolved organic matter variability in an upland forest stream. Biogeochemistry 108:183–198.

Reale, J. K., D. J. Van Horn, K. E. Condon, and C. N. Dahm. 2015. The effects of catastrophic wildfire on water quality along a river continuum. Freshwater Science 34:1426–1442.

Roberts, B. J., P. J. Mulholland, and W. R. Hill. 2007. Multiple scales of temporal variability in ecosystem metabolism rates: Results from 2 years of continuous monitoring in a forested headwater stream. Ecosystems 10:588–606.

Rode, M., A. J. Wade, M. J. Cohen, R. T. Hensley, M. J. Bowes, J. W. Kirchner, G. B. Arhonditsis, P. Jordan, B. Krongvang, S. J. Halliday, R. A. Skeffington, J. C. Rozemeijer, A. H. Aubert, K. Rinke, and S. Jomaa. 2016. Sensors in the stream: The high-frequency wave of the present. Environmental Science & Technology 50:10297–10307.

Roley, S. S., J. L. Tank, N. A. Griffiths, R. O. Hall, and R. T. Davis. 2014. The influence of floodplain restoration on whole-stream metabolism in an agricultural stream: Insights from a 5-year continuous data set. Freshwater Science 33:1043–1059.

Ruhala, S. S., and J. P. Zarnetske. 2017. Using in-situ optical sensors to study dissolved organic carbon dynamics of stream and watershed: A review. Science of the Total Environment 575: 713–723.

Sherson, L. R., D. J. Van Horn, J. D. Gomez-Velez, L. J. Crossey, and C. N. Dahm. 2015. Nutrient dynamics in an alpine headwater stream: Use of continuous water quality sensors to examine responses to wildfire and precipitation events. Hydrological Processes 29:3193–3207.

Siders, A. C., D. M. Larson, J. Ruegg, and W. K. Dodds. 2017. Probing whole-stream metabolism: Influence of spatial heterogeneity on rate estimates. Freshwater Biology 62:711–723.

Simino, J. 2002. East Fork Jemez River. Stream inventory report. Santa Fe National Forest. US Forest Service. (Available from: https://www.fs.usda.gov/Internet/FSE_DOCUMENTS/fsbdev7_020716.pdf)

Taylor, C. J., D. J. Pedregal, P. C. Young, and W. Tych. 2007. Environmental time series analysis and forecasting with the Captain toolbox. Environmental Modelling and Software 22:797–814.

Thompson, V. F., D. L. Marshall, J. K. Reale, and C. N. Dahm. 2019. The effects of catastrophic forest fire on the biomass of submerged macrophytes. Aquatic Botany 152:36–42.

Uehlinger, U. 2000. Resistance and resilience of ecosystem metabolism in a flood-prone river system. Freshwater Biology 45: 319–332.

Uehlinger, U. 2006. Annual cycle and inter-annual variability of gross primary production and ecosystem respiration in a flood-prone river during a 15-year period. Freshwater Biology 51:938–950.

Uehlinger, U., and M. W. Naegeli. 1998. Ecosystem metabolism, disturbance, and stability in a prealpine gravel bed river. Journal of the North American Benthological Society 17:165–178.

Ulseth, A. J., E. Bertuzzo, G. A. Singer, J. Schelker, and T. J. Battin. 2018. Climate-induced changes in spring snowmelt impact ecosystem metabolism and carbon fluxes in an alpine stream network. Ecosystems 21:373–390.

Val, J., D. Chinarro, M. R. Pino, and E. Navarro. 2016. Global change impacts on river ecosystems: A high-resolution watershed study of Ebro River metabolism. Science of the Total Environment 569–570:774–783.

Valett, H. M., C. N. Dahm, M. E. Campana, J. A. Morrice, M. A. Baker, and C. S. Fellows. 1997. Hydrologic influences on groundwater-surface water ecotones: Heterogeneity in nutrient composition and retention. Journal of the North American Benthological Society 16:239–247.

Van Horn, D. J., C. S. White, E. A. Martinez, C. Hernandez, J. P. Merrill, R. R. Parmenter, and C. N. Dahm. 2012. Linkages between riparian characteristics, ungulate grazing, and geomorphology and nutrient cycling in montane grassland streams. Rangeland Ecology and Management 65:475–485.

Vannote, R. L., G. W. Minshall, K. W. Cummins, J. R. Sedell, and C. E. Cushing. 1980. The river continuum concept. Canadian Journal of Fisheries and Aquatic Sciences 37:130–137.

Wagener, T., and J. Kollat. 2007. Numerical and visual evaluation of hydrological and environmental models using the Monte Carlo analysis toolbox. Environmental Modelling and Software 22:1021–1033.

Wasserstein, R. L., A. L. Schirm, and N. A. Lazar. 2019. Moving to a world beyond "$p < 0.05$". The American Statistician 73:1–19.

Young, R. G., and A. D. Huryn. 1996. Interannual variation in discharge controls ecosystem metabolism along a grassland river continuum. Canadian Journal of Fisheries and Aquatic Sciences 53:2199–2211.

Zeileis, A., and G. Grothendieck. 2005. *zoo*: S3 infrastructure for regular and irregular time series. Journal of Statistical Software 14:1–27.